MODELING AND SIMULATION OF ^{222}Rn TRANSPORT INTO ROOM AIR FROM A CONSTANT-EXHALATION CONSTANT-TEMPERATURE VERTICAL WALL

José A. Rabi
Fac. Engenharia Civil, Pontifícia Universidade Católica de Minas Gerais, campus Poços de Caldas
Av. Padre Francis Cletus Cox, 1661, Poços de Caldas, MG, 37701-355, Brazil.
Tel: + 55 – 35 – 3697 3000; Fax: + 55 – 35 – 3697 3001; E-mail: jrabi@pucpcaldas.br

Abdulmajeed A. Mohamad
Dept. Mechanical Manufacturing Engineering, Faculty of Engineering, The University of Calgary
2500 University Drive NW, Calgary, Alberta, T2N 1N4, Canada.
Tel: + 1 – 403 – 220 2781; Fax: + 1 – 403 – 282 8406; E-mail: amohamad@enme.ucalgary.ca

Abstract. *Large-scale usage of phosphogypsum – a by-product from phosphate fertilizer industry – may point to an alternative material for civil engineering. Yet, it should cope with environmental issues concerning ^{222}Rn exhalation rates. This work investigates steady-state two-dimensional ^{222}Rn transport into room air from a vertical isothermal wall assumed to exhale this radionuclide at a fixed rate. Activity decay terms are accounted for in the analysis although sources related to emanation from ^{226}Ra are not included since this radionuclide is supposedly absent in air. Natural convection is modeled under Boussinesq approximation for buoyant forces. The resulting coupled dimensionless governing equations are numerically solved following a finite-volume method on staggered orthogonal grid. Grashof number is varied from 10^6 to 10^8 and the corresponding effects on heat and mass transfers are presented. For the set of controlling parameters adopted for this particular ^{222}Rn problem, decay effects are of minor importance.*

Keywords*: Natural convection, Finite-volume method, Phosphogypsum, Radon exhalation.*

1. INTRODUCTION

Huge amounts of phosphogypsum have been by-produced worldwide as a result of demands for phosphate fertilizers (Rutherford et al., 1994). Both large-scale utilization of this by-product (e.g. alternative building material and soil amendment in agriculture) and its embankment and/or stack disposal have given rise to environmental issues as far as ^{222}Rn exhalation rates are concerned.

The effective dose owing to ^{222}Rn and its short-lived decay products counts for most of human exposure to radiation from natural sources (UNSCEAR, 2000). Such radioactive gas results from the α-decay of ^{226}Ra, an impurity commonly found in phosphogypsum. Therefore, ^{226}Ra present in phosphogypsum-bearing materials decay to ^{222}Rn, which may percolate through the interstices, reach up the free surface and be inhaled by nearby humans. A reliable model for ^{222}Rn transport can then be useful for radiation exposure assessment as well as for radiological protection design.

Several physical parameters influence the ^{222}Rn transport since different phases may be involved in the simultaneous processes of emanation, adsorption, absorption, diffusion, convection and decay. Accordingly, a comprehensive model is likely to become complex and the nuclear physicist or engineer should then rely on numerical simulation.

A previous work presented a diffusion-dominated mathematical model for ^{222}Rn transport through phosphogypsum embankments in dimensionless form (Rabi and Mohamad, 2004). The model was limited to one-dimensional steady-state transport and natural convective effects were ignored. Three dimensionless groups arose in the analytical solution process, namely, an emanation-to-diffusion ratio, a decay-to-diffusion ratio and a surrogate emanation-to-decay ratio.

The present paper intends to alter that aforementioned work twofold: by extending the solution domain up to two-dimensions and by considering natural convection. The problem investigated is of an isothermal vertical wall which contains a given amount of phosphogypsum and exhales ^{222}Rn at constant rate into room air whose temperature is lower.

It is assumed that air density variations are due to thermal effects only (i.e., negligible solutal effects due to mass transfer), following Boussinesq hypothesis for the buoyancy driven air flow. The analysis considers decay rates although activity source terms are not included. The resulting coupled partial differential equations are written in dimensionless form and numerically solved following a finite-volume method on a staggered orthogonal grid.

2. PHYSICAL-MATHEMATICAL MODEL

2.1. Primitive Variables Formulation

Figure 1 shows the Cartesian coordinate system and the schematic diagram of the problem under investigation. The solution domain is a rectangle of height H (m) and width L (m).

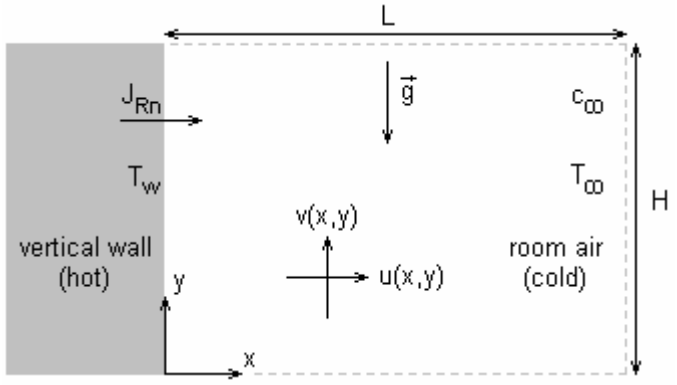

Figure 1. Schematic diagram and coordinate system for natural convective transport of ^{222}Rn over a constant-exhalation constant-temperature vertical wall.

Natural convection under Boussinesq approximation is assumed for the air laminar flow. Hence, all thermo-physical properties are supposed to be constant, except for the density ρ (kg·m^{-3}) in the buoyant forces in the y-direction momentum equation, for which a linear dependence on local temperature T (K) is assumed, namely,

$$\rho(T) = \rho_\infty[1 - \beta(T - T_\infty)] \tag{1}$$

where $\beta = \rho_\infty^{-1}(\partial\rho/\partial T)_\infty$ (K^{-1}) is the coefficient of thermal volumetric expansion and both density ρ_∞ and temperature T_∞ are reference state values.

Indicating u and v (m·s^{-1}) as velocity components in x and y directions respectively, p (Pa) as pressure, υ (m^2·s^{-1}) as kinematic viscosity, g (m·s^{-2}) as acceleration due to gravity, α (m^2·s^{-1}) as thermal diffusivity, λ (s^{-1}) as ^{222}Rn decay constant, D_o (m^2·s^{-1}) and c (Bq·m^{-3}) respectively as ^{222}Rn diffusivity and activity concentration in open air, the steady-state governing equations for mass, momentum, energy and species (^{222}Rn activity) concentration can be written respectively as

$$\frac{\partial u}{\partial x} + \frac{\partial v}{\partial y} = 0 \tag{2}$$

$$u\frac{\partial u}{\partial x} + v\frac{\partial u}{\partial y} = \upsilon\left(\frac{\partial^2 u}{\partial x^2} + \frac{\partial^2 u}{\partial y^2}\right) - \frac{1}{\rho_\infty}\frac{\partial p}{\partial x} \tag{3}$$

$$u\frac{\partial v}{\partial x} + v\frac{\partial v}{\partial y} = \upsilon\left(\frac{\partial^2 v}{\partial x^2} + \frac{\partial^2 v}{\partial y^2}\right) - \frac{1}{\rho_\infty}\frac{\partial p}{\partial y} + g\beta(T - T_\infty) \tag{4}$$

$$u\frac{\partial T}{\partial x} + v\frac{\partial T}{\partial y} = \alpha\left(\frac{\partial^2 T}{\partial x^2} + \frac{\partial^2 T}{\partial y^2}\right) \tag{5}$$

$$u\frac{\partial c}{\partial x} + v\frac{\partial c}{\partial y} = D_o\left(\frac{\partial^2 c}{\partial x^2} + \frac{\partial^2 c}{\partial y^2}\right) - \lambda c \tag{6}$$

In Eq. (6), $-\lambda c$ is a sink term but no source terms since it is assumed that room air lacks ^{226}Ra. This radionuclide is supposed to be evenly distributed inside the wall as a phosphogypsum impurity, yielding a fixed activity flux J_{Rn} (Bq·m^{-2}·s^{-1}) into room air. Because such mass flux is very small compared to the entire air mass content, solutal variations in the bulk density ρ_∞ can be neglected.

Boundary conditions for the previous governing equations include no-slip condition at the wall ($x = 0$), which is subjected to constant temperature T_w and exhalation rate J_{Rn}. Sufficiently far from the wall ($x = L$), air is assumed to be at rest and at fixed temperature $T_\infty < T_w$ and to exhibit activity concentration c_∞. These last two conditions are also assumed at the lower wall level ($y = 0$), where neither momentum back-flow nor fluid cross-flow are allowed. At the wall upper level ($y = H$), a free boundary condition is prescribed for all primitive unknown variables. Mathematically,

$$x = 0: \qquad u = v = 0 \qquad T = T_w = const \qquad J_{Rn} = -D_o\frac{\partial c}{\partial x} = const \tag{7}$$

$$x = L: \qquad u = v = p = 0 \qquad T = T_\infty = const \qquad c = c_\infty = const \tag{8}$$

$$y = 0: \qquad u = \frac{\partial v}{\partial y} = p = 0 \qquad T = T_\infty = const \qquad c = c_\infty = const \tag{9}$$

$$y = H: \qquad \frac{\partial u}{\partial y} = \frac{\partial v}{\partial y} = p = 0 \qquad \frac{\partial T}{\partial y} = 0 \qquad \frac{\partial c}{\partial y} = 0 \tag{10}$$

2.2. Dimensionless Governing Equations and Boundary Conditions

Governing equations, Eqs. (2) to (6), and related boundary conditions, Eqs. (7) to (10), can be conveniently expressed in dimensionless form. Accordingly, the following dimensionless variables are defined:

$$X = \frac{x}{H} \;,\; Y = \frac{y}{H} \;,\; U = \frac{uH}{\upsilon} \;,\; V = \frac{vH}{\upsilon} \;,\; P = \frac{pH^2}{\rho\upsilon^2} \;,\; \theta = \frac{T - T_\infty}{T_w - T_\infty} \;,\; \phi = \frac{D_o(c - c_\infty)}{J_{Rn} H} \quad (11)$$

Introduction of the above definitions into Eqs. (2) to (10) leads to the following expressions:

$$\frac{\partial U}{\partial X} + \frac{\partial V}{\partial Y} = 0 \quad (12)$$

$$U\frac{\partial U}{\partial X} + V\frac{\partial U}{\partial Y} = \frac{\partial^2 U}{\partial X^2} + \frac{\partial^2 U}{\partial Y^2} - \frac{\partial P}{\partial X} \quad (13)$$

$$U\frac{\partial V}{\partial X} + V\frac{\partial V}{\partial Y} = \frac{\partial^2 V}{\partial X^2} + \frac{\partial^2 V}{\partial Y^2} - \frac{\partial P}{\partial Y} + \mathrm{Gr}^*\theta \quad (14)$$

$$U\frac{\partial \theta}{\partial X} + V\frac{\partial \theta}{\partial Y} = \frac{1}{\mathrm{Pr}}\left(\frac{\partial^2 \theta}{\partial X^2} + \frac{\partial^2 \theta}{\partial Y^2}\right) \quad (15)$$

$$U\frac{\partial \phi}{\partial X} + V\frac{\partial \phi}{\partial Y} = \frac{1}{\mathrm{Sc}}\left(\frac{\partial^2 \phi}{\partial X^2} + \frac{\partial^2 \phi}{\partial Y^2}\right) - \frac{\mathrm{R}}{\mathrm{Sc}}(\phi - \phi_0) \quad (16)$$

$$X = 0: \qquad U = V = 0 \qquad \theta = 1 \qquad \frac{\partial \phi}{\partial X} = -1 \quad (17)$$

$$X = \mathrm{A}: \qquad U = V = P = 0 \qquad \theta = 0 \qquad \phi = 0 \quad (18)$$

$$Y = 0: \qquad U = \frac{\partial V}{\partial Y} = P = 0 \qquad \theta = 0 \qquad \phi = 0 \quad (19)$$

$$Y = 1: \qquad \frac{\partial U}{\partial Y} = \frac{\partial V}{\partial Y} = P = 0 \qquad \frac{\partial \theta}{\partial Y} = 0 \qquad \frac{\partial \phi}{\partial Y} = 0 \quad (20)$$

Dimensionless parameters that characterize the physics of the problem are the aspect ratio A, Prandtl number Pr, Schmidt number Sc, Grashof number Gr, a so-called decay-to-diffusion ratio R and a dimensionless activity concentration level ϕ_0. These are defined respectively as

$$\mathrm{A} = \frac{L}{H} \;,\; \mathrm{Pr} = \frac{\upsilon}{\alpha} \;,\; \mathrm{Sc} = \frac{\upsilon}{D_o} \;,\; \mathrm{Gr} = \frac{g\beta(T_w - T_\infty)H^3}{\upsilon^2} \;,\; \mathrm{R} = \frac{\lambda H^2}{D_o} \;,\; \phi_0 = \frac{-D_o c_\infty}{J_{Rn} H} \quad (21)$$

The above expression for the decay-to-diffusion ratio R may result from the definition suggested in (Rabi and Mohamad, 2004) by simply setting the so-called partition-corrected porosity to unity.

With respect to the last of Eqs. (11), it is observed that the dimensionless activity level ϕ_0 is the value for ϕ when $c = 0$. It is then assumed $c_\infty = 0$ so that $\phi_0 = 0$ and Eq. (16) can be rewritten as

$$U\frac{\partial \phi}{\partial X} + V\frac{\partial \phi}{\partial Y} = \frac{1}{\mathrm{Sc}}\frac{\partial^2 \phi}{\partial X^2} + \frac{1}{\mathrm{Sc}}\frac{\partial^2 \phi}{\partial Y^2} - \frac{\mathrm{R}}{\mathrm{Sc}}\phi \quad (22)$$

2.3. Local and Average Rate of Heat and Mass Transfer

The rate of heat and mass transfer across the vertical wall is expressed in dimensionless form by means of the Nusselt and Sherwood numbers respectively. For the problem under investigation, the latter is a measure of the average ^{222}Rn activity transferred into room air.

By defining a local heat transfer coefficient h_y (W·m^{-2}·K^{-1}) according to

$$\dot{q}''_w = h_y (T_w - T_\infty) \quad \Leftrightarrow \quad h_y = \frac{\dot{q}''_w}{T_w - T_\infty} \tag{23}$$

and evoking Fourier's law of heat conduction, one can express the local Nusselt number Nu_y, with the help of Eqs. (11), as follows

$$\mathrm{Nu}_y = \frac{h_y y}{k} = \frac{-y}{T_w - T_\infty}\left(\frac{\partial T}{\partial x}\right)_w \quad \Rightarrow \quad \mathrm{Nu}_y = -Y\left(\frac{\partial \theta}{\partial X}\right)_{X=0} \tag{24}$$

The average heat transfer coefficient h and the average Nusselt number Nu are evaluated as

$$h = \frac{1}{H}\int_0^H h_y \, \mathrm{d}y = -\frac{k}{H}\int_0^1 \left(\frac{\partial \theta}{\partial X}\right)_{X=0} \mathrm{d}Y \quad \Rightarrow \quad \mathrm{Nu} = \frac{hH}{k} = -\int_0^1 \left(\frac{\partial \theta}{\partial X}\right)_{X=0} \mathrm{d}Y \tag{25}$$

Similarly, a local ^{222}Rn activity transfer coefficient γ_y (m·s^{-1}) can be defined as

$$J_{Rn} = \gamma_y (c_w - c_\infty) \quad \Leftrightarrow \quad \gamma_y = \frac{J_{Rn}}{c_w - c_\infty} \tag{26}$$

where c_w is the ^{222}Rn activity concentration at the wall. By evoking Fick's law of diffusion and again recalling Eqs. (11), the local Sherwood number Sh_y can be expressed as

$$\mathrm{Sh}_y = \frac{\gamma_y y}{D_o} = \frac{J_{Rn}}{(c_w - c_\infty)}\frac{y}{D_o} \quad \Rightarrow \quad \mathrm{Sh}_y = \frac{Y}{\phi_w} = \frac{Y}{\phi_{X=0}} \tag{27}$$

Expressions for average ^{222}Rn activity transfer coefficient γ and average Sherwood number Sh are

$$\gamma = \frac{1}{H}\int_0^H \gamma_y \, \mathrm{d}y = \frac{D_o}{H}\int_0^1 \frac{1}{\phi_w}\mathrm{d}Y = \frac{D_o}{H}\int_0^1 \frac{1}{\phi_{X=0}}\mathrm{d}Y \quad \Rightarrow \quad \mathrm{Sh} = \frac{\gamma H}{D_o} = \int_0^1 \frac{1}{\phi_w}\mathrm{d}Y = \int_0^1 \frac{1}{\phi_{X=0}}\mathrm{d}Y \tag{28}$$

3. NUMERICAL METHOD

This work adapted an existing finite-volume simulator which has been successfully used for the solution of heat and mass transfer problems in porous media (Mohamad, 2003). Equations (12) to (15) and (22) are converted into a system of algebraic equations after integration over each control volume in the solution domain. As a preliminary approach, uniformly spaced meshes were used.

Staggered grid arrangement is adopted so as to prevent pressure oscillations. Algebraic equations are solved iteratively and velocity components are under-relaxed by a factor of 0.7 whereas other relaxation factors are set to unity. Convergence criteria are based on local and global conservation of mass, momentum, energy and species within pre-selected error tolerances.

In order to ensure that results are grid size independent, 8000 iterations were performed on the following meshes: 162 × 82, 202 × 102, 252 × 127 and 302 × 152. Controlling parameters adopted for a test case were A = 2, Pr = Sc = 1, Gr = 10^6 and R = 0. It should be noted that by inserting the latter value in Eq. (22), the ^{222}Rn activity transfer problem becomes similar to that of a vertical wall subjected to constant heat flux. Hence, the corresponding heat-mass transfer analogy holds.

Table 1(*a*) compares numerical results obtained for Nu_y at $Y = 1$, as calculated by Eq. (24), to values from correlations for free convection over a uniform temperature vertical wall (Ede, 1967; LeFreve, 1956; McAdams, 1954; Eckert, 1950). Table 1(*b*) shows simulated results for Sh_y at $Y = 1$, as calculated by Eq. (27), and values for Nu_y taken from correlations for free convection over a constant heat flux vertical wall (Fujii and Fujii, 1976; Vliet, 1969; Vliet and Liu, 1969). This latter comparison stems from a heat-mass transfer analogy, as discussed in the preceding paragraph.

Table 1. Comparison between numerical results and values computed from correlations for (*a*) local Nusselt number Nu_y and (*b*) local Sherwood number Sh_y, both at $Y = 1$.

(*a*) Local Nusselt number Nu_y at $Y = 1$							
Numerical result from grid size of				Computed value as suggested by			
162 × 82	202 × 102	252 × 127	302 × 152	Ede	LeFreve	McAdams	Eckert
15.58517	15.25721	14.93420	14.66468	12.61345	12.67163	13.99308	13.59076

(*b*) Local Sherwood number Sh_y at $Y = 1$					
Numerical result from grid size of				Computed value (for Nu_y) as suggested by	
162 × 82	202 × 102	252 × 127	302 × 152	Fujii and Fujii	Vliet and Liu
19.32559	18.88084	18.46145	18.12191	14.48468	16.27068

Differences between predictions for either successive Nu_y or Sh_y remain at approximately 2% or less, following the above grid size refinement sequence. Numerical values differ from those given by correlations possibly due to edge effects. As calculations on the 302 × 152 grid demand a considerable computational effort, results shown in this work were obtained using the 252 × 127 grid. It is worth mentioning that correlations from (Fujii and Fujii, 1976; Vliet, 1969; Vliet and Liu, 1969) are based on the modified local Grashof number, $Gr_y^* = Gr_y \cdot Nu_y$. In this case, the required local Nusselt number Nu_y was taken from numerical results on the 302 × 152 grid.

4. NUMERICAL RESULTS AND DISCUSSION

Representative values for ^{222}Rn transport problems are $D_o \cong 1.1 \times 10^{-5}$ m^2·s^{-1} (Yu et al., 1993) and $\lambda = 2.098 \times 10^{-6}$ s^{-1} (UNSCEAR, 2000). For that reason, the present investigation is limited to the following controlling parameters: A = 2, Pr = 0.71 (room air), Sc = 1.36 (as from D_o above and $\upsilon \cong 1.5 \times 10^{-5}$ m^2·s^{-1} for room air) and R = 0.01. The Grashof number is allowed to vary within the range $10^6 \le Gr \le 10^8$.

Figures 2 and 3 show the dimensionless V and U profiles, respectively, at $Y = 1$ for Gr = 10^6, 10^7 and 10^8. Although full Navier-Stokes equations are being numerically solved, Eqs. (12) to (14), the simulator was able to reproduce the basic features of a free-convection boundary-layer flow over a vertical wall under Boussinesq approximation. Large values are particularly observed for V because velocity components are normalized by υ/H, which is quite small. Identical profiles are obtained for the same set of controlling parameters but assuming R = 0 instead. These profiles are not presented for clarity. This behavior is expected as it was assumed that ^{222}Rn mass flux causes no substantial changes to the bulk air density.

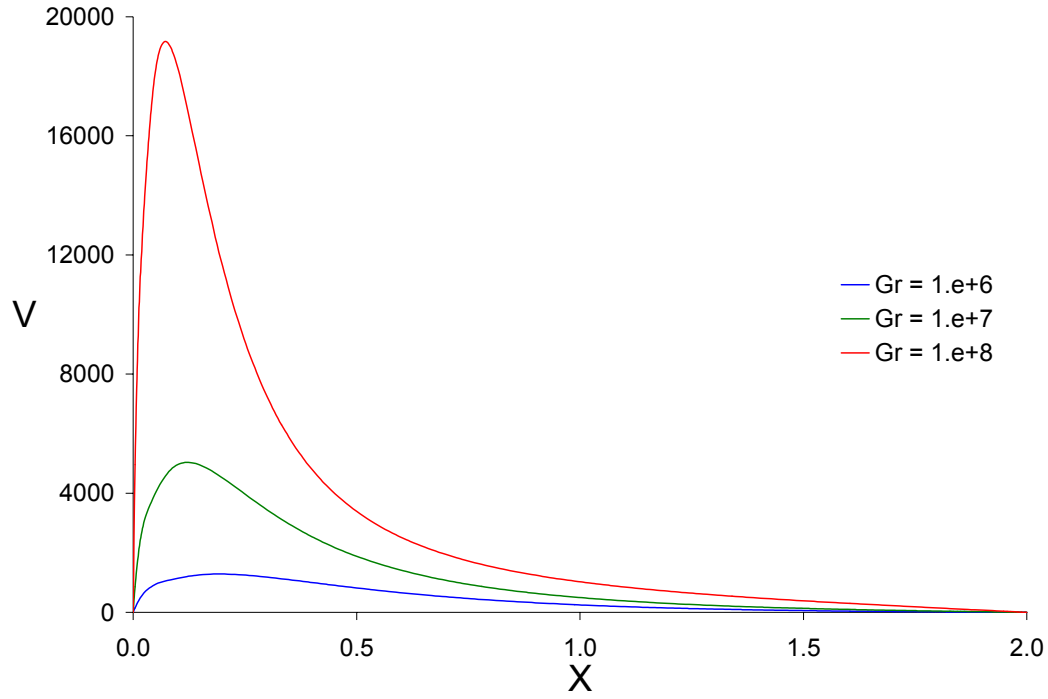

Figure 2. Profiles for the dimensionless V velocity component at $Y = 1$.

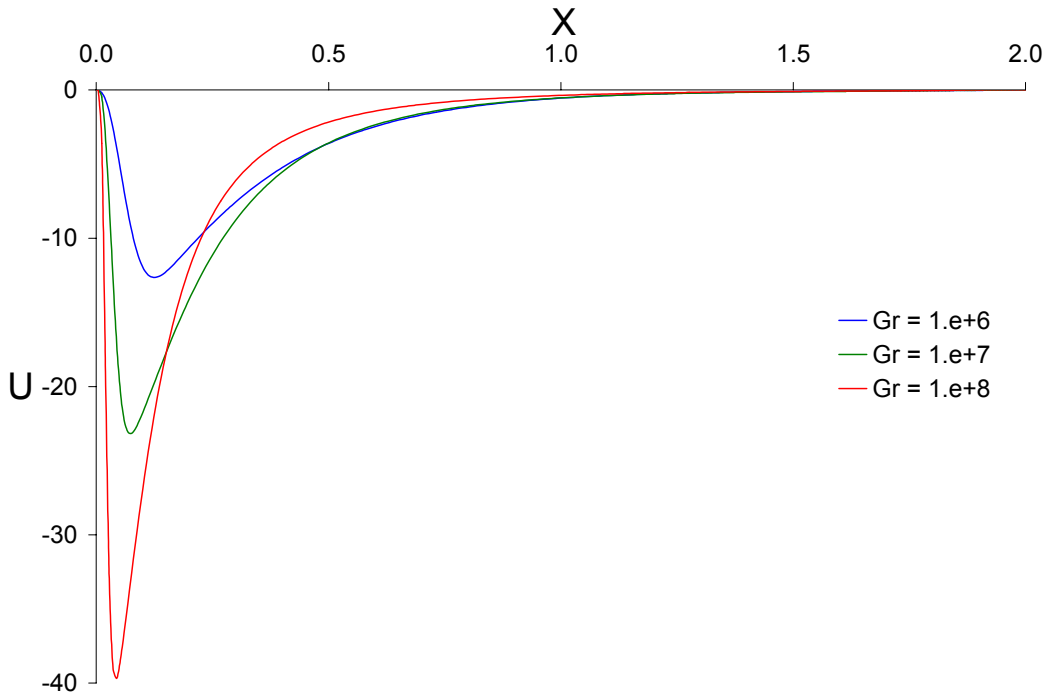

Figure 3. Profiles for the dimensionless U velocity component at $Y = 1$.

Figure 4 exhibits the dimensionless temperature θ profiles at $Y = 1$ for Gr = 10^6, 10^7 and 10^8. Similar to what happens to V and U, identical θ profiles are obtained for both R = 0.01 and R = 0 (profiles for R= 0 are not shown for clarity). This is also expected for the same rationale discussed in the previous paragraph. It should be noted that only an initial portion of the X domain is presented (instead of the whole $0 \leq X \leq$ A representation) since all θ profiles drop to zero within a short range.

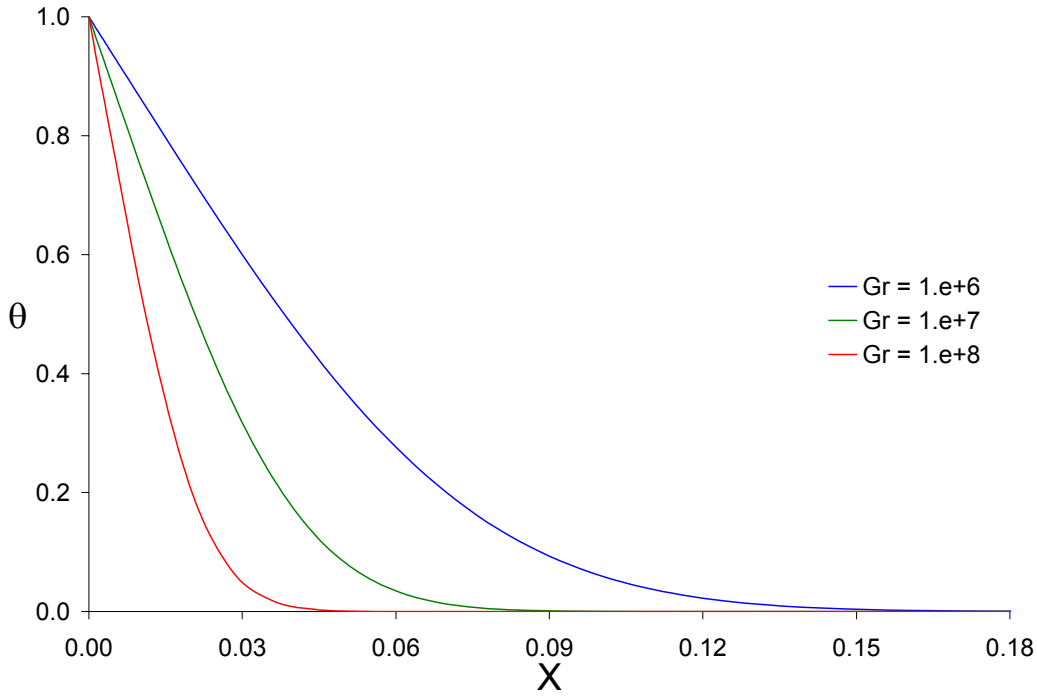

Figure 4. Profiles for the dimensionless temperature θ at $Y = 1$.

Figure 5 explicitly shows the dimensionless ^{222}Rn activity concentration ϕ profiles at $Y = 1$ for both R = 0.01 and R = 0 for Gr = 10^6, 10^7 and 10^8. Analogous to θ profiles, only an initial portion of the X domain is presented as all ϕ profiles drop to zero within a short range. It is also worth noting that the fixed exhalation rate at the wall, last of Eqs. (17), was satisfactorily reproduced.

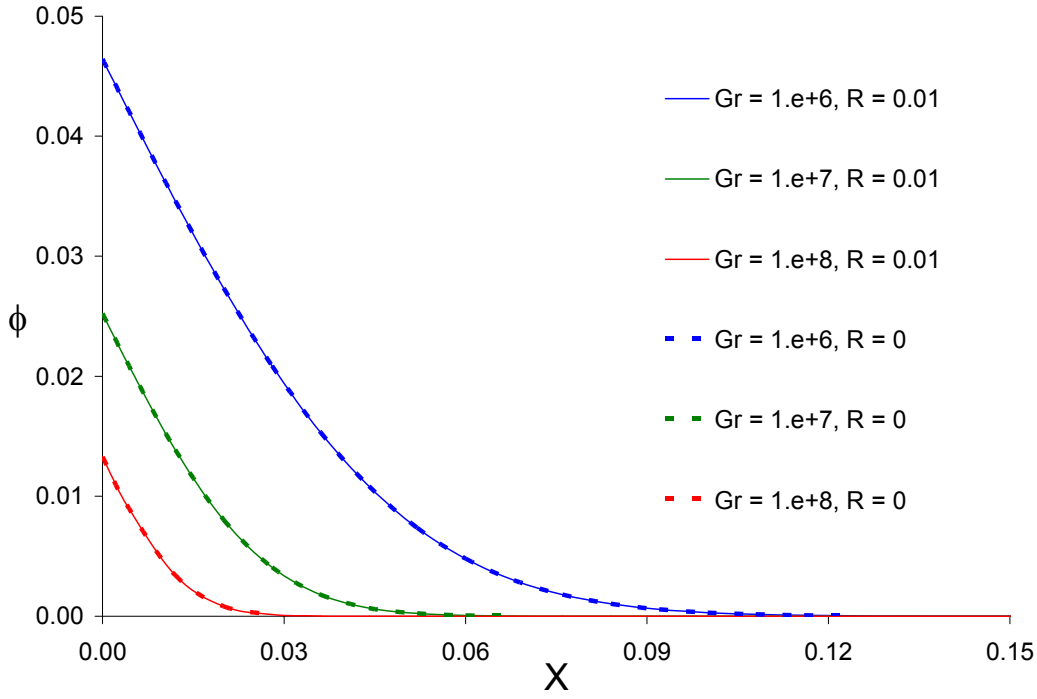

Figure 5. Profiles for the dimensionless ^{222}Rn activity concentration ϕ at $Y = 1$.

Despite of the additional sink (decay) term in Eq. (22), no considerable differences are observed between profiles from simulations using R = 0.01 and R = 0. This can be explained in terms of the

relatively small decay-to-diffusion parameter suggested by the physical problem under investigation (R = 0.01), which makes decay effects become negligible. Larger values of R (and hence decay effects) are likely to be found in ^{222}Rn transport across long distances H, e.g. across the atmosphere (Piliposian and Applebly, 2003), or through porous media where lower diffusivity D can be found (Yu et al., 1993; UNSCEAR, 2000).

Finally, Fig. 6 plots both the average Nusselt and Sherwood numbers obtained from simulations using R = 0.01, as evaluated respectively according to Eqs. (25) and (28), for Grashof numbers in the range $10^6 \leq Gr \leq 10^8$. Results show that the ascending profiles for Nu and Sh with respect to Gr are virtually parallel in a log-log scale. The upward natural convective flow field increases inasmuch as Grashof number becomes higher and such more intense air movement seems to enhance heat and mass transfers basically in the same way.

It is worth bearing in mind that air is assumed to have constant temperature T_∞ ($\theta = 0$) and ^{222}Rn activity concentration c_∞ ($\phi = 0$) at the lower level ($y = Y = 0$), Eqs. (9) and (19). Such conditions demand special analysis as far as a closed cavity (i.e. room) is concerned. All previous results refer to a limited portion of an isothermal constant-exhalation vertical wall. No attempts were made as to analyze effects due to windows, fans or opposing and/or adjacent walls in the present investigation.

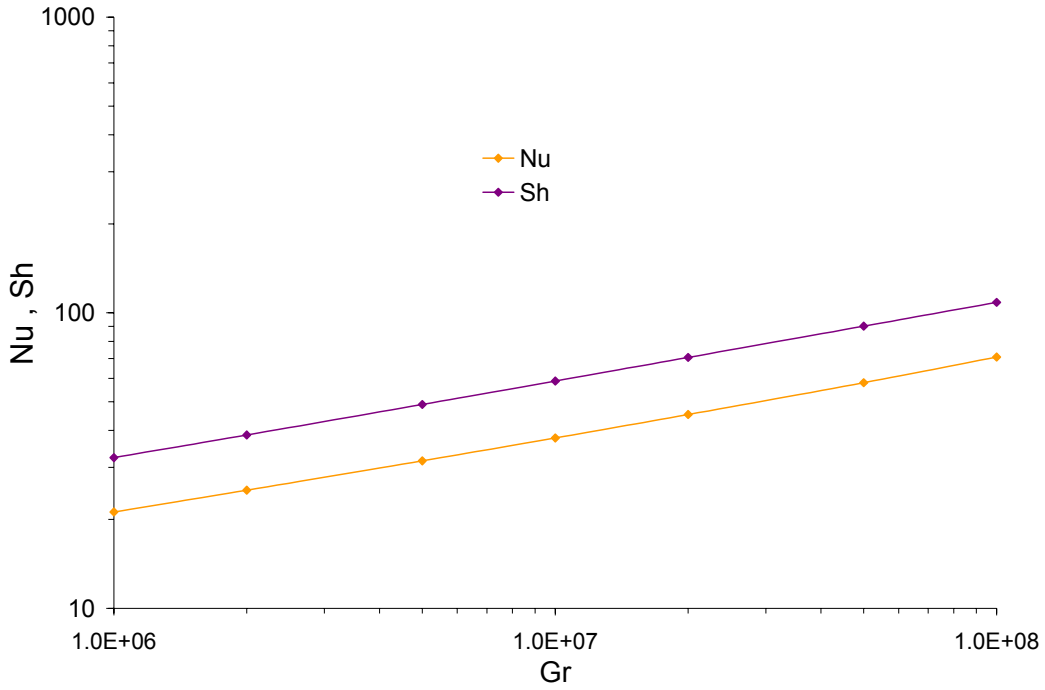

Figure 6. Average Nusselt and Sherwood numbers as function of Grashof number for R = 0.01.

5. CONCLUDING REMARKS

A section of a constant-temperature constant-exhalation rate vertical wall was investigated. Radon activity penetrates into room air whose ascending laminar buoyancy-driven flow is assumed to follow Boussinesq approximation. Despite full Navier-Stokes equations were numerically solved, boundary conditions were adopted in order to simulate satisfactorily the expected free convection flow field over an isothermal vertical wall.

Decay (sink) rates were taken into account but ^{222}Rn activity source terms were not included. In accordance to a previous definition, the decay-to-diffusion ratio R proved to be relatively small for the controlling parameters adopted. Numerical results showed no considerable changes if compared to those obtained assuming a similar mass transfer scenario without the decay term. In other words,

the ^{222}Rn transfer investigated showed a diffusive dominant nature under the assumptions made. It is presumed that decay effects should be observed in problems corresponding to higher values of R.

It was found that heat and mass transfer rates are enhanced by increasing the Grashof number. Activity concentration results were numerically obtained assuming that the incoming fluid (i.e., air arriving at the lower wall level) exhibits a constant reference value c_∞. Means to guarantee such condition should then be provided or designed.

6. ACKNOWLEDGEMENT

The first author is grateful to CAPES (Coordenação de Aperfeiçoamento de Pessoal de Nível Superior, Brazil) for the financial support (Process BEX 0624/03-9).

7. REFERENCES

Eckert, E.R., 1950, "Introduction to the Transfer of Heat and Mass", McGraw-Hill, New York.

Ede, A.J., 1967, "Advances in Heat Transfer", vol. 4, Academic Press, New York.

Fujii, T. and Fujii, M., 1976, Int. J. Heat Mass Transfer, vol. 19, pp. 121-122.

LeFreve, E.J., 1956, "Laminar free convection from a vertical plane surface", Proc. 9th Int. Congr. Applied Mechanics, Brussels, vol. 4, pp. 168-174.

McAdams, W.H., 1954, "Heat Transmission", 3rd ed., McGraw-Hill, New York.

Mohamad, A.A., 2003, "Heat transfer enhancements in heat exchangers fitted with porous media. Part I: constant wall temperature", Int. J. Thermal Sciences, vol. 42, pp. 385-395.

Piliposian, G.T. and Appleby, P.G., 2003, "A simple model of the origin and transport of ^{222}Rn and ^{210}Pb in the atmosphere", Continuum Mech. Thermodyn., vol. 15, pp. 503-518.

Rabi, J.A. and Mohamad, A.A., 2004, "A parametric approach for the prediction of ^{222}Rn exhalation rates from phosphogypsum-based embankments", Proceedings of ICAPM 2004 – International Conference on Applications of Porous Media, May 24-27, Evora, Portugal.

Rutherford, P.M., Dudas, M.J. and Samek, R.A., 1994, "Environmental impacts of phosphogypsum", Science of the Total Environment, vol. 149, pp. 1-38.

UNSCEAR – United Nations Scientific Committee on the Effects of Atomic Radiation, 2000, "Sources and effects of ionizing radiation", New York, U.N.

Vliet, G.C., 1969, "Natural convection local heat transfer on constant-heat-flux inclined surfaces", J. Heat Transfer, vol. 91C, pp. 511-516.

Vliet, G.C. and Liu, C.K., 1969, "An experimental study of natural convection boundary layers", J. Heat Transfer, vol. 91C, pp. 517-531.

Yu, C., Loureiro, C., Cheng, J.-J., Jones, L.G., Wang, Y.Y., Chia, Y.P. and Faillace, E., 1993, "Data Collection Handbook to Support Modeling Impacts of Radioactive Materials in Soil", Argonne National Laboratory, Argonne, Illinois.